24. Joutel, A. *et al.* Notch3 mutations in CADASIL, a hereditary adult-onset condition causing stroke and dementia. *Nature* **383**, 707–710 (1996).
25. Cao, X. & Sudhof, T. A. Transcriptively active complex of APP with Fe65 and histone actyltransferase Tip60. *Science* **293**, 115–120 (2001).
26. Gusella, J. F. & MacDonald, M. E. Molecular genetics: unmasking polyglutamine triggers in neurodegenerative disease. *Nature Rev. Neurosci.* **1**, 109–115 (2000).
27. Marsh, J. L. *et al.* Expanded polyglutamine peptides alone are intrinsically cytotoxic and cause neurodegeneration in *Drosophila*. *Hum. Mol. Genet.* **9**, 13–25 (2000).
28. Zuccato, C. *et al.* Loss of huntingtin-mediated BDNF gene transcription in Huntington's disease. *Science* **293**, 493–498 (2001).
29. Yuasa, T. *et al.* Joseph's disease: clinical and pathologic studies in a Japanese family. *Ann. Neurol.* **19**, 152–157 (1986).
30. Ikeda, H. *et al.* Expanded polyglutamine in the Machado–Joseph disease protein induces cell death *in vitro* and *in vivo*. *Nature Genet.* **13**, 196–202 (1996).
31. Warrick, J. M. *et al.* Expanded polyglutamine protein forms nuclear inclusions and causes neural degeneration in *Drosophila*. *Cell* **93**, 939–949 (1998).
32. The Huntington's Disease Collaborative Research Group. A novel gene containing a trinucleotide repeat that is expanded and unstable on Huntington's disease chromosomes. *Cell* **72**, 971–983 (1993).
33. DiFiglia, M. *et al.* Aggregation of huntingtin in neuronal intranuclear inclusions and dystrophic neurites in brain. *Science* **277**, 1990–1993 (1997).
34. Jackson, G. R. *et al.* Polyglutamine-expanded human huntingtin transgenes induce degeneration of *Drosophila* photoreceptor neurons. *Neuron* **21**, 633–642 (1998).
35. Steffan, J. S. *et al.* Histone deacetylase inhibitors arrest polyglutamine-dependent neurodegeneration in *Drosophila*. *Nature* **413**, 739–743 (2001).
36. Fernandez-Funez, P. *et al.* Identification of genes that modify ataxin-1-induced neurodegeneration. *Nature* **408**, 101–106 (2000).
37. Warrick, J. M. *et al.* Suppression of polyglutamine-mediated neurodegeneration in *Drosophila* by the molecular chaperone HSP70. *Nature Genet.* **23**, 425–428 (1999).
38. Chan, H. Y. E., Warrick, J. M., Gray-Board, G. L., Paulson, H. L. & Bonini, N. M. Mechanisms of chaperone suppression of polyglutamine disease: selectivity, synergy and modulation of protein solubility in *Drosophila*. *Hum. Mol. Genet.* **9**, 2811–2820 (2000).
39. Auluck, P. K., Chan, H. Y. E., Trojanowski, J. Q., Lee, V. M.-Y. & Bonini, N. M. Chaperone suppression of α-synuclein toxicity in a *Drosophila* model for Parkinson's disease. *Science* 20 December 2001 (10.1126/science.1067389).
40. Kazemi-Esfarjani, P. & Benzer, S. Genetic suppression of polyglutamine toxicity in *Drosophila*. *Science* **287**, 1837–1840 (2000).
41. McCampbell, A. *et al.* CREB-binding protein sequestration by expanded polyglutamine. *Hum. Mol. Genet.* **9**, 2197–2202 (2000).
42. Davidson, F. F. & Stellar, H. Blocking apoptosis prevents blindness in *Drosophila* retinal degeneration mutants. *Nature* **391**, 587–591 (1998).
43. Lewis, J. *et al.* Enhanced neurofibrillary degeneration in transgenic mice expressing mutant tau and APP. *Science* **293**, 1487–1491 (2001).
44. Gotz, J., Chen, J., Van Dorpe, J. & Nitsch, R. M. Formation of neurofibrillary tangles in P301L tau transgenic mice induced by Aβ42 fibrils. *Science* **293**, 1491–1495 (2001).
45. Elia, A. J. *et al.* Expression of human FALS SOD in motoneurons of *Drosophila*. *Free Radic. Biol. Med.* **26**, 1332–1338 (1999).
46. Raeber, A. J., Muramoto, T., Kornberg, T. B. & Prusiner, S. B. Expression and targeting of Syrian hamster prion protein induced by heat shock in transgenic *Drosophila melanogaster*. *Mech. Dev.* **51**, 317–327 (1995).
47. Kitada, T. *et al.* Mutations in the parkin gene cause autosomal recessive juvenile parkinsonism. *Nature* **392**, 605–608 (1998).
48. Yamamoto, A., Lucas, J. J. & Hen, R. Reversal of neuropathology and motor dysfunction in a conditional model of Huntington's disease. *Cell* **101**, 57–66 (2000).
49. Osterwalder, T., Yoon, K. S., White, B. H. & Keshishian, H. A conditional tissue-specific transgene expression system using inducible GAL4. *Proc. Natl Acad. Sci. USA* **98**, 12596–12601 (2001).
50. Stebbins, M. J. *et al.* Tetracycline-inducible systems for *Drosophila*. *Proc. Natl Acad. Sci. USA* **98**, 10775–10780 (2001).
51. Min, K.-T. & Benzer, S. Preventing neurodegeneration in the *Drosophila* mutant *bubblegum*. *Science* **284**, 1985–1988 (1999).
52. Van Geel, B. M. *et al.* Progression of abnormalities in adrenomyeloneuropathy and neurologically asymptomatic X-linked adrenoleukodystrophy despite treatment with 'Lorenzo's oil'. *J. Neurol. Neurosurg. Psychiatry* **67**, 290–299 (1999).
53. Kretzschmar, D., Hasan, G., Sharma, S., Heisenberg, M. & Benzer, S. The *swiss cheese* mutant causes glial hyperwrapping and brain degeneration in *Drosophila*. *J. Neurosci.* **17**, 7425–7432 (1997).
54. Min, K. T. & Benzer, S. Spongecake and eggroll: two hereditary diseases in *Drosophila* resemble patterns of human brain degeneration. *Curr. Biol.* **7**, 885–888 (1997).
55. Buchanan, R. L. & Benzer, S. Defective glia in the *Drosophila* brain degeneration mutant *drop-dead*. *Neuron* **10**, 839–850 (1993).
56. Eberl, D. F., Duyk, G. M. & Perrimon, N. A genetic screen for mutations that disrupt an auditory response in *Drosophila melanogaster*. *Proc. Natl Acad. Sci. USA* **94**, 14837–14842 (1997).
57. Bennett, C. L. & Chance, P. F. Molecular pathogenesis of hereditary motor, sensory and autonomic neuropathies. *Curr. Opin. Neurol.* **14**, 621–627 (2001).

Online links

DATABASES

The following terms in this article are linked online to:

FlyBase: http://flybase.bio.indiana.edu/
Appl | *bubblegum* | CtBP | *dishevelled* | DnaJ-1 | *drop dead* | *eggroll* | *elav* | *GMR* | Notch | *parkin* | *pirouette* | Rpd3 | Sin3A | Sir2 | *spongecake* | *swiss cheese* | Tpr2

LocusLink: http://www.ncbi.nlm.nih.gov/LocusLink/
APP | ataxin 1 | ataxin 3 | CBP | HDJ1 | HSP70 | huntingtin | *NOTCH3* | parkin | presenilin 1 | presenilin 2 | prion protein | superoxide dismutase | α-synuclein | TAU | TRP2

OMIM: http://www.ncbi.nlm.nih.gov/Omim/
ALD | ALS | Alzheimer's disease | CADASIL | Charcot–Marie–Tooth disease | Creutzfeldt–Jakob disease | FTDP-17 | Huntington's disease | Parkinson's disease | retinitis pigmentosa | SCA-1 | SCA-3

***Saccharomyces* Genome Database:**
http://genome-www.stanford.edu/Saccharomyces/
GAL4

FURTHER INFORMATION

Encyclopedia of Life Sciences:
http://www.els.net/
Alzheimer disease | Huntington disease | Morgan, Thomas Hunt | Parkinson disease

Access to this interactive links box is free online.

OPINION

The problem of functional localization in the human brain

Matthew Brett, Ingrid S. Johnsrude and Adrian M. Owen

Functional imaging gives us increasingly detailed information about the location of brain activity. To use this information, we need a clear conception of the meaning of location data. Here, we review methods for reporting location in functional imaging and discuss the problems that arise from the great variability in brain anatomy between individuals. These problems cause uncertainty in localization, which limits the effective resolution of functional imaging, especially for brain areas involved in higher cognitive function.

In the past ten years, rapid improvements in imaging technology and methodology have had an enormous impact on how we assess human cognition. Detailed anatomical images can be combined with functional images that are obtained using techniques such as positron emission tomography (PET) and functional magnetic resonance imaging (fMRI) to address questions that relate to normal and abnormal brain function. A chief advantage of techniques such as fMRI and PET over methods such as electroencephalography, magnetoencephalography and neuropsychology is their ability to localize changes in brain activity with a high degree of spatial resolution. In this article, we will argue that specifying where in the brain an activation has occurred is both conceptually and technically more difficult than has been generally assumed.

Processing steps in functional imaging

A functional imaging study involves the collection of one or more functional scans for each subject, which show signal changes in regions where neuronal work has increased (FIG. 1). To compensate for subject movement, it is usual to realign the functional images to one of the images in the series. Most investigators collect a separate structural scan that has good spatial resolution to image the anatomy of the brain. The structural scan may have a different field of view, voxel size or orientation, so that it will need to be coregistered to the functional images using an automated image-matching algorithm.

There are now two possible approaches to the analysis. The first is to proceed directly to the statistical analysis. This approach maintains a very clear relationship between the subject's anatomy and activation. Many researchers prefer the second approach, which

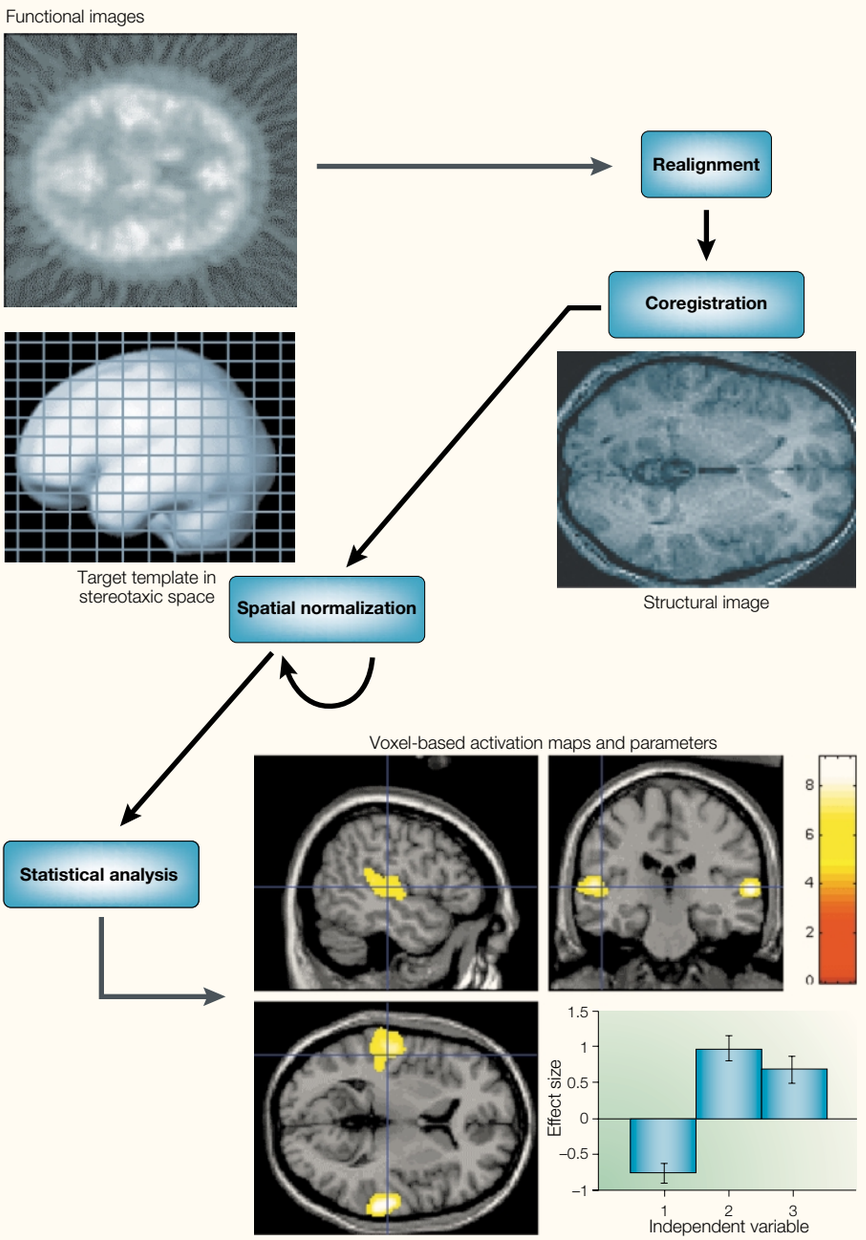

Figure 1 | **Stages of image processing.** The functional images for each subject are realigned to correct for subject movement, and then coregistered with a structural image. If required, the images are spatially normalized to align brains across subjects. Statistical analysis attempts to detect areas that have been activated by the experimental manipulation. The results can be displayed on individual or average structural images.

is to do the statistical analysis after transforming the images for each subject to match a template brain, such as that described by Talairach and Tournoux (BOX 1). This makes it easier to compare the signal location with other subjects and studies that have been similarly transformed.

Spatial normalization is the process of transforming an image for an individual subject to match a standard brain or brain template. Many investigators use an automated distortion method to match the overall shape of the structural image to a structural template, such as that provided by the Montreal Neurological Institute (MNI; BOX 2). Once the transformations have been calculated for the structural image, they are applied to the functional images using the correspondence found by coregistration.

Statistical analysis may involve any of a number of methods[1], most of which result in some index at each voxel of how the brain has responded to the experimental manipulation of interest. This activation map can be thresholded to identify activated brain regions. If we have scanned several subjects, then we can do intersubject averaging to find regions that respond on average across subjects. The estimate of location of an activation will be subject to some error due to statistical noise[2].

The final step of the analysis is labelling of the activated areas. The labels may be in terms of stereotaxic coordinates, macroanatomy, microanatomy or function. Coordinate labels are obtained using a standard coordinate system, such as that introduced by Talairach and Tournoux (BOX 1). Macroanatomical labels relate the activation to gyri/sulci on the cortex or to deep brain nuclei. Microanatomical labels specify where the activation is in terms of a parcellation of the brain that reflects microscopic features of the cortex. In practice, the parcellation is almost always based on cytoarchitecture — differences in cell types and distributions within the layers of the cortex[3–5]. Functional labels are based on a parcellation into areas that have been defined functionally — for example, in other imaging studies.

Activation labelling and spatial normalization are the two key steps that are involved in localization. The success of these steps will determine our ability to compare results across individuals and studies.

Activation labelling

Early functional imaging studies concentrated on primary and secondary sensorimotor areas, for which activation labelling is relatively straightforward. If we have collected fMRI data during a task that involves finger movement, and overlaid the activation due to movement on the structural image, we are likely to see an activation in the anterior bank of the central sulcus (FIG. 2). In this case, labelling the activation is not controversial, because anatomical, functional and cytoarchitectonic labels are highly related. The anatomical location — the anterior bank of the central sulcus — contains a functional area, the motor cortex, that has been identified by physiological and anatomical techniques. And the motor cortex corresponds closely to a cytoarchitectonic area (Brodmann area (BA) 4)[6].

The situation is less straightforward in many other brain areas. A working memory task is likely to activate the frontal cortex[7] (FIG. 2). In this case, it is difficult to know what label to allocate to a particular activation. The

Box 1 | **The atlas of Talairach and Tournoux**

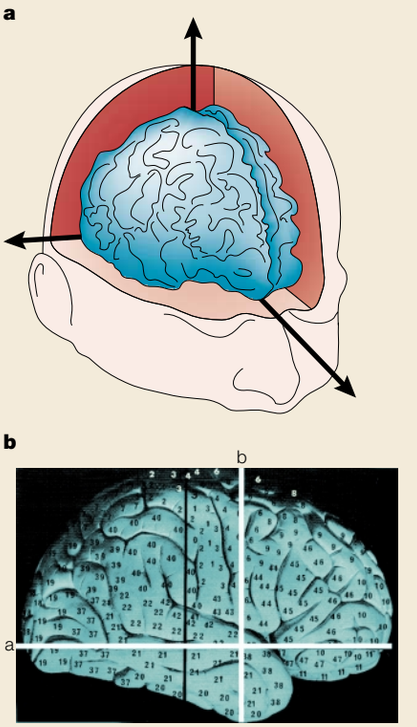

Talairach and Tournoux[65] published a stereotaxic atlas of the human brain that has been enormously influential in functional imaging. They introduced three important innovations: a coordinate system to identify a particular brain location relative to anatomical landmarks; a spatial transformation to match one brain to another; and an atlas describing a standard brain, with anatomical and cytoarchitectonic labels.

The type of coordinate system that Talairach and Tournoux introduced has become almost universal in functional imaging. The authors suggested that the brain should be aligned according to the anterior commissure (AC) and posterior commissure (PC) — two small subcortical structures that are relatively invariant. The brain is rotated so that the interhemispheric fissure is on a vertical plane. The experimenter draws a line between the AC and PC (the AC–PC line), and rotates the brain so that this line is on a horizontal plane. Now, we can define a coordinate relative to three orthogonal axes, with the AC as the origin (panel **a**). The *y* axis is the AC–PC line ('a' in panel **b**; reproduced with permission from REF. 65 © 1988 Thieme Medical Publishers); the *z* axis is a vertical line that passes through the interhemispheric fissure and the AC ('b' in panel **b**); and the *x* axis is a horizontal line at right angles to the *y* and *z* axes that passes through the AC. We can identify any point in the brain relative to these axes, which define the Talairach coordinate system.

The atlas also described a simple set of scalings (the proportional grid system) that can be used to transform one brain to give a rough match to another in overall brain size and shape. There are different scalings for different brain quadrants. We first align the brains to the Talairach axes, defined above, then scale the brain between the AC and the PC so that the distance between these commissures is the same in the two brains. Similarly, we scale the distances between the AC and the top, bottom and sides of the brain, and between the PC and the back of the brain. This transformation is termed the Talairach proportional grid normalization.

The main part of the atlas is a series of labelled diagrams of transverse (axial), sagittal and coronal brain slices from the post-mortem brain of a 60-year-old French woman (the 'Talairach brain'). The brain is oriented according to the Talairach axes; a coordinate in a brain that has been transformed according to the proportional grid system should match the same coordinate location in the atlas slices. Only one hemisphere is given in any detail, and so symmetry must be assumed. Talairach and Tournoux labelled the brain slices with anatomical labels, including important sulci and gyri. They also estimated the Brodmann cytoarchitectonic areas for the cortical surface (numbers on the surface of the brain in panel **b**). They based their estimate only on a comparison of the gross anatomy of the Talairach brain with the well-known map published by Brodmann[3], and did not mark the borders of the Brodmann areas. To quote from the atlas: "The brain presented here was not subjected to histological studies and the transfer of the cartography of Brodmann usually pictured in two dimensional projections sometimes possesses uncertainties."

sulcal morphology of the prefrontal cortex is highly variable, so it is difficult to choose an anatomical label that will be meaningful for all subjects. The cytoarchitecture of the prefrontal cortex is complex, and there is little agreement on the boundaries of cytoarchitectonic fields or how cytoarchitecture relates to sulcal anatomy. There is no consensus on the fractionation of functions within the prefrontal cortex[7]. So, it is difficult to decide whether we should label an activation by macroscopic anatomy, cytoarchitecture or function; and if we label according to cytoarchitecture or function, it is difficult to choose the area to which the activation corresponds.

Coordinate labels. If a researcher has spatially normalized their data, they will often report a stereotaxic coordinate for the activations, usually in relation to the Talairach coordinate system (BOX 1). The coordinate chosen to represent an activated area is typically that with the highest level of activation. A coordinate is often the most useful label for comparison with other results in neuroimaging. The accuracy with which we can compare coordinates will depend on the similarity of the images, templates and normalization techniques used (see our discussion of meta-analysis and location error, below). An important problem with coordinate labels is that it can be difficult to compare coordinates with brain locations obtained from other types of data, such as those arising from work on non-human primates. Stereotaxic coordinates can also be misleading, compared with surface coordinates, if the location is near a deep sulcus, because a small change in the coordinate can correspond to a large change in distance across the cortical surface[8].

Macroanatomical labels. Macroanatomical labels relate the activation to cortical sulci or deep brain nuclei. As the main use of labels is to identify an activation as belonging to a functional area, macroanatomical labels are of most use when there is an established relationship between anatomy and function. This is usually the case for the deep brain nuclei, but the relationship of function to sulcal anatomy is much less clear. It is reasonable to identify motor cortex activation according to its position in relation to the central sulcus. The same applies to primary auditory cortex, which has a clear relationship with Heschl's gyrus, and to primary visual cortex, which can be identified by the position of the calcarine sulcus. These sulci and gyri are relatively invariant in position and configuration between individuals. However, most sulci in the brain are highly variable between subjects[9] and even between hemispheres in a single subject. Evidence from cytoarchitecture indicates that sulci that are constant in position and morphology between individuals can reflect functional subdivisions, but this might not be the case for sulci that are present in only some individuals, or sulci that have a very different morphology in different subjects[10]. This rule is not invariable; Watson *et al.*[11] have shown that V5, the visual motion area, is well defined by the posterior end of the inferior temporal sulcus, even though this sulcus shows a considerable degree of variation between individuals.

Box 2 | **The MNI/ICBM templates**

The Montreal Neurological Institute (MNI) created a series of images similar to the Talairach brain that were based on the average of many normal magnetic resonance imaging (MRI) scans. Such images can be used by automated spatial normalization software, and should reflect average neuroanatomy. The International Consortium of Brain Mapping (ICBM) has adopted these templates as an international standard.

The first MNI template, MNI305, was created using a two-stage process[66]. The first stage was manual scaling to the Talairach brain: 241 brains were oriented and scaled to the Talairach brain using manually defined landmarks[67]. The first-pass image was the average of these reoriented/rescaled brains[68]. The MNI305 template is the average of 305 normal MRI scans that have been normalized to the first-pass image by an automated linear normalization[69]. The current standard MNI template is known as the ICBM152, and is based on 152 brains that were registered to MNI305; this template is provided with several commonly used functional imaging analysis packages, including the Statistical Parametric Mapping package SPM99, and the FMRIB Software Library (FSL). The MNI also created a high-quality image of a single individual that was based on an average of 27 scans. This image, known as colin27, has been normalized to MNI305 and was used as a template in the 1996 release of SPM software.

Although the MNI template is based on the Talairach brain, the two brains are not exactly the same size or shape; in particular, the temporal lobes in the MNI template extend ~10 mm below those of the Talairach brain. The differences between the MNI template and the Talairach brain have been a source of confusion in the neuroimaging community, as they have not always been recognized. Software packages such as SPM report coordinates of activations registered to the MNI template as 'Talairach coordinates', because the coordinates are relative to axes that are very similar to those defined by Talairach. Such coordinates do not refer directly to the Talairach brain, because of the differences between the Talairach brain and the MNI template. As yet, there is no published estimate of Brodmann areas that correspond to the anatomy of the MNI template. Many researchers use coordinates from the MNI template to look up estimated Brodmann areas in the Talairach atlas. If the differences are not accounted for, this can lead to significant errors, especially for coordinates in the temporal lobe. One approach has been to estimate by eye which area in the atlas corresponds to the coordinate in the MNI template; another has been to use a transformation for coordinates from the MNI template that matches the brains more closely. See the MRC Cognition and Brain Sciences Unit website for a discussion of the MNI brain and the Talairach atlas (http://www.mrc-cbu.cam.ac.uk/Imaging/mnispace.html).

Microanatomical labels. Microanatomy refers to the connectivity, neurotransmitters and cytoarchitecture of the layers of the cortex. For technical reasons, microanatomical studies in humans are rare and connectivity analyses are extremely difficult. Cytoarchitecture continues to be widely used for several reasons. First, cell-staining techniques reveal regional variations in the laminar distribution and morphology of cells that often correlate with regional specialization of function. Second, the results can be directly related to a large database that spans more than 100 years. Finally, the techniques are more robust than most histochemical and immunohistochemical treatments, producing more reliable results even after extended post-mortem delays and suboptimal tissue treatment. So, despite providing limited information about functional organization, cytoarchitecture remains, for pragmatic reasons, the main microanatomical indicator of functional specificity.

Cytoarchitecture generally correlates well with parcellation schemes that are based on other kinds of anatomical description, when compared in humans and other primates[12–16]. However, parcellations that are based on cytoarchitecture have seldom been compared systematically with histochemistry or connectivity in areas outside the primary cortex in any species. It seems likely that such correspondences will not always hold: different parcellation schemes may apply when different markers are used. For example, in auditory cortex, researchers have found areas that with some markers seem to be primary, but with other markers do not (see REFS 17,18; see REF. 19 for a proposal on how to tackle similar issues). Further complexity is added by the fact that even primary areas, which are homogeneous at one level of analysis, are heterogeneous at another. In the primary visual cortex (V1), a stain for cell bodies reveals laminar, alternating stripes of cell-dense and cell-sparse cortex. Cytochrome oxidase is expressed patchily over the surface of V1 in 'blobs' that are associated functionally with colour and motion analysis; inputs from the left and right eye alternate over the surface of the field; and sensitivity to line orientation also changes in an orderly way over V1 (REF. 20). As more is learned about other cortical areas, we should expect similarly complex patterns to emerge. Despite this complexity, anatomical factors must influence function, and relating functional activation to microanatomical structure might be very valuable.

Most studies of human cytoarchitecture indicate that, although there is substantial variability in both the size and location of cytoarchitectonic fields among individuals[4,5,13,21–23], many distinguishable fields do have some relationship to gross sulcal and gyral morphology. Primary visual cortex is always found within the calcarine sulcus, although it generally extends somewhat onto the free surface of the occipital lobe. However, calcarine sulcal depth is indicative of the total volume of primary visual cortex[24]. Primary auditory cortex always covers at least a portion of the first transverse temporal gyrus (of Heschl)[22,25]. Even though, again, extents of overlap are variable and areal extents vary markedly between hemispheres and between individuals, this area never reaches the lateral aspect of the superior temporal gyrus, and probability maps of Heschl's gyrus[26] and cytoarchitectonically defined primary auditory cortex[22] overlap substantially[22,27]. Even in what might be considered as higher-order areas, outside primary thalamocortical target zones, a degree of predictability of architectonic areas from gross morphological features is found. Area 44 in the inferior frontal gyrus (part of classical Broca's area) varies in size by an order of magnitude across individuals. However, the location of the dorsal border of this area, although variable, is always within the inferior frontal sulcus and never appears on the lateral aspect of the middle frontal gyrus[21]. Sulci that have great variability in position and morphology might have less constant relationships to cytoarchitecture[10,23].

The convention of relating activation foci to Brodmann cytoarchitectonic areas was adopted early in functional imaging. These labels are usually assigned by reference to the Talairach brain (BOX 1), either by direct comparison to the atlas or by using an online database[28]. Talairach and Tournoux estimated the position of the Brodmann areas by comparing the published Brodmann map with the surface of the brain described in the atlas. So, there are several ways in which BA assignment on the basis of Talairach coordinates could be erroneous: first, cytoarchitectonic area extent and location could be inaccurate on the Talairach brain; second, the spatially normalized sample image might be misregistered with the space of the Talairach

atlas; and third, the variability in location and extent of cytoarchitectonic areas across individuals implies that BA assignment on the basis of binary information (coordinate *x,y,z* is either in area A or it is not) is prone to error unless cytoarchitectonic data are available on the sample image. How can we improve our ability to localize foci relative to cytoarchitectonic parcellation?

Karl Zilles and colleagues have undertaken architectonic analyses of several areas in post-mortem human brains. Importantly, high-resolution MRI scans of the brains are taken before histological processing. After semi-automated, quantitative microscopic analysis of the slices, an architectonic parcellation over slices is developed; the architectonic profiles of individual slices can then be digitized and registered with the MRI scan[29]. Three-dimensional cytoarchitectonic volumes have been created in this way for various anatomical areas, including primary somatosensory[30–32], motor[33], visual[34] and auditory[22] areas, as well as Broca's area[21]. As these volumes are coregistered to structural MRIs, the same whole-brain normalization can be carried out on the post-mortem data as is applied to functional data, ensuring a close match between the two. If we assume that the subjects used are representative of the population, then the location of a cytoarchitectonic area can be estimated by averaging over the individual, spatially normalized volumes of the region. In such an average, the value at any voxel codes the likelihood that that voxel is located in that area. This kind of probabilistic approach compensates for variability in sulcal and gyral morphology after normalization, and the use of cytoarchitectonic information in such probabilistic maps gives a measure of variability in location and extent of cytoarchitectonic areas over subjects[35]. For examples of this approach, see REFS 36–38.

Of course, it would be better to localize activations relative to a subject's own microstructural anatomy than to rely on estimates of anatomy derived from other individuals. New techniques might allow this. Diffusion tensor imaging is an MRI technique that is sensitive to white matter connectivity; such information is already being used to a limited extent to inform the analysis of functional imaging data[39–41]. Cortical laminar thickness and composition have been examined in monkeys using high-field MRI and surface coils to enhance spatial resolution. Such studies seem to provide much of the information that traditional post-mortem cell-staining studies have offered, opening the way to *in vivo* architectonic mapping[42–44].

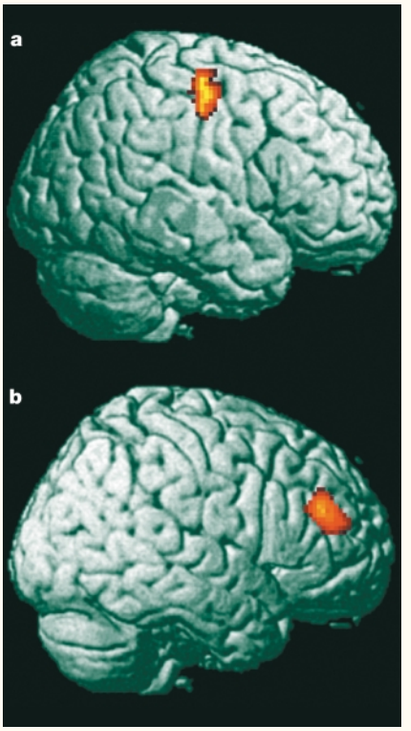

Figure 2 | **Examples of activation maps superimposed on the subject's structural image. a** | Activation arising from a motor task is focused on the anterior bank of the central sulcus. **b** | Activation arising from a working memory task is located in the prefrontal cortex.

Functional labels. An alternative approach to functional parcellation is to locate presumed functional units using functional imaging experiments, and to use the positions of these areas to label activation.

This approach is particularly powerful in single-subject analyses. For example, using fMRI, Kanwisher and colleagues have identified four specific areas of the temporal lobe that respond when subjects view faces, objects, scenes or body parts[45–47]. Their subsequent strategy has been to start a functional imaging session with an experiment in which subjects view these types of stimulus to identify the functional area of interest. They then use the areas that have been identified to analyse data from other experiments on the same subject. For example, Epstein *et al.*[48] used such a task to identify the area that responds to scenes; they then investigated whether activation in this area could be explained on the basis of memory encoding. So, this approach can be used to identify the functional area of interest on the basis of the subject's own anatomy, avoiding the problem of inaccurate overlap of functional areas by spatial normalization.

Problems of spatial normalization

Normalization is closely related to activation labelling. Successful normalization requires a strong conception of how brain anatomy corresponds to function, because it is usually designed to give the best spatial correspondence of homologous areas between individuals. Normalization also affects labelling that is based on information from a template brain; if the normalization does not succeed in aligning corresponding functional areas, then definitions of functional areas from other individuals will not be applicable.

How we try to match two brains will depend on our idea of how anatomy is likely to relate to function. For example, if we believe that the sulci are a useful guide to the position of functional areas, then we can use a warping method that aligns the sulci between two brains. If not, we might prefer a more restricted solution that matches the size and outline of the brain.

Some volume-matching algorithms, such as the Talairach proportional grid normalization (BOX 1), use manually identified landmarks to find the best scaling parameters. Most current methods include automated image-matching algorithms[49]. These methods use a mathematical measure of overall image mismatch and a minimization algorithm with iterative changes in transformations to find the best set of transformations to match the image to the template. Usually, they begin by optimizing linear parameters: translations, rotations, zooms and often shears. They then proceed to find the best set of nonlinear (warping) parameters to further match the detail of brain shape[50,51]. Volume-matching methods contain no model of the cortical surface, and are not usually designed to provide detailed matching of sulcal anatomy between subjects (but see REF. 29).

Sulcal-matching methods attempt an explicit match of sulcal anatomy between subjects. The user first extracts a model of the cortical surface from the structural image. The algorithms then distort this model of the cortical surface so that it matches the template. The algorithms need to be constrained so that prominent invariant sulci drive the matching more strongly than variable features[8,49,52,53]. As expected, these methods seem to be better than volume-matching algorithms at overlapping functional areas near invariant sulci, such as visual and motor areas[52]. Unfortunately, many areas of interest might not have consistent relationships with sulci, and it is not clear which method is better for these areas. Sulcal methods involve the estimation of activation signal on the cortical surface. This can be very sensitive to problems in coregistration of the

functional and structural images, so sulcal normalization might inflate small errors. Because of problems with magnetic field inhomogeneity, coregistration errors are a particular problem for fMRI[54]. If function does not clearly correspond to a particular sulcus, then sulcal matching can provide a worse match of function than the volume method. Further work on warping methods is likely to combine surface and volume matching to give a good match across a range of cortical and subcortical brain areas[49].

The researcher is likely to choose the normalization method that gives the best overlap of the functional areas of interest. Functional areas that are well defined by sulci are likely to be best aligned using surface normalization. For most functional areas, such as those in the prefrontal cortex, there is little evidence on which to base a decision; volume methods are often chosen because they are simpler and faster to apply.

The purpose of normalization should be to bring homologous areas into the closest possible alignment, but this can be difficult to assess, because we do not have a gold standard against which to compare[55]. To assess the alignment of homologous areas, we need some estimate of the corresponding areas in the brains that are to be normalized. This is likely to become available as more areas are mapped cytoarchitectonically on brains that can be spatially normalized[6]. For example, Roland *et al.*[35] compared the Talairach proportional grid normalization with a linear and a nonlinear manual technique, and showed that the latter was more effective in overlapping cytoarchitectonic maps from post-mortem brains. An alternative is to use a battery of tasks that give a highly reproducible activation pattern across subjects. A normalization technique can be assessed by its ability to overlay the areas of activation.

The success of normalization in overlapping homologous areas is important for intersubject averaging; if functional areas are not well aligned between individuals, then there might appear to be no location at which there is an average increase in activation, even if all subjects have activated a homologous region. The problem of intersubject averaging becomes even more acute when comparing differences in functional anatomy between groups. For example, we might use intersubject averaging to find that controls activate the dorsolateral frontal cortex more than do patients with schizophrenia. Interpreting this finding might be confounded by differences in anatomy between the two groups. For example, it is possible that each individual patient with schizophrenia had activated the dorsolateral frontal cortex normally, but that subtle differences in anatomy between the patients and controls had resulted in a less successful overlap of the dorsolateral frontal cortex for the patients. On this basis, one might conclude that there was a functional difference between the groups in frontal cortex activation, when in fact the difference was anatomical.

> "The success of activation labelling and normalization will dictate our ability to compare results between imaging studies."

Normalization also determines the effective spatial resolution of a study that involves a direct comparison across subjects; homologous areas that have been successfully overlapped will have a higher resolution than areas for which the overlap has been less successful, so effective resolution might differ considerably across different functional areas.

One approach to the problem of imperfect alignment of functional areas across individuals is to use image smoothing, so that the activation for each subject is blurred across a larger area. This can result in greater overlap of activation when comparing across subjects, but has the disadvantage that it reduces spatial resolution. If the activated areas are not well matched, group average activation can be diffuse even if the activation was highly localized for the individual subjects.

Meta-analysis and location error

The success of activation labelling and normalization will dictate our ability to compare results between imaging studies. The most powerful way to compare studies is to do a direct statistical comparison, but this is possible only if we have the original data. Often, we are faced with the task of doing an implicit or explicit meta-analysis of imaging studies[56]. In this case, we need to compare the positions of the activations that are observed in different studies, and this can be done only with reported location labels. Because gross anatomy does not correlate well with function outside the main sulci, these labels are usually not helpful for meta-analysis. Similarly, a cytoarchitectonic label can be derived from one of several sources, which might differ in their estimation of the area corresponding to a given location. Even if the source of information on cytoarchitecture is the same for two studies, the estimation of which area the activation belongs to is to some extent subjective. For these reasons, meta-analyses usually include coordinates in a stereotaxic space as the labels of interest.

Coordinates in stereotaxic space can be difficult to compare. Although an increasing number of investigators use the MNI templates (BOX 2), many use local templates or match directly to the Talairach brain. If studies adopt different templates, coordinates will not be directly comparable. A transformation might be needed to match between templates[57], which involves further potential for inaccuracy. If we have used a different template or a different normalization method, then the transformations calculated by the normalization might differ in a systematic way. Differences in the contrast or signal-to-noise of images that are used for normalization might result in differences in the success of normalization. There will also be some statistical error in the estimation of location; this error will differ across studies and is rarely quantified. So, meta-analysis might have low spatial resolution and power; this resolution will differ for different brain areas. However, for some areas, it can be shown that activations in similar tasks do correspond across studies (for examples, see REFS 7,56,58,59).

False-negative findings can be a problem when comparing across studies. We are often faced with the situation of deciding whether it is true that a task has not activated a particular area. This is a question of statistical power, which is complex in standard imaging analyses[60,61]. Most imaging analyses have low power[62,63]; the power depends on the intensity of the noise, which will vary from study to study, and from voxel to voxel. So, it can be very difficult to conclude with confidence that there is no activation of a given magnitude within a brain area.

Often, we wish to know whether the activations reported in one task are in different locations from those reported in a second task. The problem then arises of comparing one set of coordinate locations with another. This can be addressed using statistical methods[58,64].

Conclusion

In this article, we have argued that for imaging to advance we need to have a clear concept of localization. We are only slowly beginning to standardize parcellations of the brain in terms of function and microanatomy. Current methods of matching different brains cannot eliminate differences in functional areas across individuals, because the positions of these areas are not well predicted by gross anatomical landmarks in many regions. These problems, as well as statistical and practical issues to do with spatial processing and brain templates, mean that there are many barriers

to comparing localization across individuals and studies with any degree of accuracy. We need an integrated idea of the relationship between brain structure and function to be able to improve localization in areas outside the primary motor and sensory cortices.

Matthew Brett, Ingrid S. Johnsrude and Adrian M. Owen are at the MRC Cognition and Brain Sciences Unit, 15 Chaucer Road, Cambridge CB2 2EF, UK.
Correspondence to M.B.
e-mail: matthew.brett@mrc-cbu.cam.ac.uk

DOI: 10.1038/nrn756

1. Worsley, K. J. An overview and some new developments in the statistical analysis of PET and fMRI data. *Hum. Brain Mapp.* **5**, 254–258 (1997).
2. Grabowski, T. J. *et al.* Reliability of PET activation across statistical methods, subject groups, and sample sizes. *Neuroimage* **4**, 23–46 (1996).
3. Brodmann, K. *Vergleichende Lokalisationslehre der Grosshimrinde in ihren Prinzipien dargestellt auf Grund des Zellenbaues* (Barth, Leipzig, 1909).
4. von Economo, C. & Koskinas, G. N. *Die cytoarchitectonic der Hirnrinde des erwachsenen Menschen* (Springer, Berlin, 1925).
5. Sarkissov, S. A. *et al.* (eds) *Atlas of the Cytoarchitectonics of the Human Cerebral Cortex* (Medgiz, Moscow, 1955).
6. Roland, P. E. & Zilles, K. Brain atlases — a new research tool. *Trends Neurosci.* **17**, 458–467 (1994).
7. Owen, A. M. The role of the lateral frontal cortex in mnemonic processing: the contribution of functional neuroimaging. *Exp. Brain Res.* **133**, 33–43 (2000).
8. Fischl, B. *et al.* High-resolution intersubject averaging and a coordinate system for the cortical surface. *Hum. Brain Mapp.* **8**, 272–284 (1999).
9. Ono, M., Kubik, S. & Abernathey, C. D. *Atlas of the Cerebral Sulci* (Thieme Medical, New York, 1990).
10. Tzourio-Mazoyer, N. *et al.* in *Handbook of Medical Imaging: Processing and Analysis* (ed. Bankman, I.) 449–463 (Academic, San Diego, 2000).
11. Watson, J. D. *et al.* Area V5 of the human brain: evidence from a combined study using positron emission tomography and magnetic resonance imaging. *Cereb. Cortex* **3**, 79–94 (1993).
12. Kotter, R. *et al.* Multimodal characterisation of cortical areas by multivariate analyses of receptor binding and connectivity data. *Anat. Embryol. (Berl.)* **204**, 333–350 (2001).
13. Roland, P. E. & Zilles, K. Structural divisions and functional fields in the human cerebral cortex. *Brain Res. Brain Res. Rev.* **26**, 87–105 (1998).
14. Morel, A., Garraghty, P. E. & Kaas, J. H. Tonotopic organization, architectonic fields, and connections of auditory cortex in macaque monkeys. *J. Comp. Neurol.* **335**, 437–459 (1993).
15. Kaas, J. H. & Hackett, T. A. Subdivisions of auditory cortex and processing streams in primates. *Proc. Natl Acad. Sci. USA* **97**, 11793–11799 (2000).
16. Rivier, F. & Clarke, S. Cytochrome oxidase, acetylcholinesterase, and NADPH-diaphorase staining in human supratemporal and insular cortex: evidence for multiple auditory areas. *Neuroimage* **6**, 288–304 (1997).
17. Morosan, P. *et al.* Human primary auditory cortex: cytoarchitectonic subdivisions and mapping into a spatial reference system. *Neuroimage* **13**, 684–701 (2001).
18. Wallace, M. N., Johnston, P. W. & Palmer, A. R. Histochemical identification of cortical areas in the auditory region of the human brain. *Exp. Brain Res.* (in the press).
19. Amunts, K. & Zilles, K. Advances in cytoarchitectonic mapping of the human cerebral cortex. *Neuroimaging Clin. N. Am.* **11**, 151–169 (2001).
20. Kaas, J. H. & Collins, C. E. The organization of sensory cortex. *Curr. Opin. Neurobiol.* **11**, 498–504 (2001).
21. Amunts, K. *et al.* Broca's region revisited: cytoarchitecture and intersubject variability. *J. Comp. Neurol.* **412**, 319–341 (1999).
22. Rademacher, J. *et al.* Probabilistic mapping and volume measurement of human primary auditory cortex. *Neuroimage* **13**, 669–683 (2001).
23. Rajkowska, G. & Goldman-Rakic, P. S. Cytoarchitectonic definition of prefrontal areas in the normal human cortex: II. Variability in locations of areas 9 and 46 and relationship to the Talairach Coordinate System. *Cereb. Cortex* **5**, 323–337 (1995).
24. Gilissen, E. & Zilles, K. The calcarine sulcus as an estimate of the total volume of human striate cortex: a morphometric study of reliability and intersubject variability. *J. Hirnforsch.* **37**, 57–66 (1996).
25. Rademacher, J. *et al.* Topographical variation of the human primary cortices: implications for neuroimaging, brain mapping, and neurobiology. *Cereb. Cortex* **3**, 313–329 (1993).
26. Penhune, V. B. *et al.* Interhemispheric anatomical differences in human primary auditory cortex: probabilistic mapping and volume measurement from magnetic resonance scans. *Cereb. Cortex* **6**, 661–672 (1996).
27. Hall, D. A. *et al.* Spectral and temporal processing in human auditory cortex. *Cereb. Cortex* **12**, 140–149 (2002).
28. Lancaster, J. L. *et al.* Automated Talairach atlas labels for functional brain mapping. *Hum. Brain Mapp.* **10**, 120–131 (2000).
29. Schormann, T. & Zilles, K. Three-dimensional linear and nonlinear transformations: an integration of light microscopical and MRI data. *Hum. Brain Mapp.* **6**, 339–347 (1998).
30. Geyer, S., Schleicher, A. & Zilles, K. The somatosensory cortex of human: cytoarchitecture and regional distributions of receptor-binding sites. *Neuroimage* **6**, 27–45 (1997).
31. Geyer, S., Schleicher, A. & Zilles, K. Areas 3a, 3b, and 1 of human primary somatosensory cortex. *Neuroimage* **10**, 63–83 (1999).
32. Geyer, S. *et al.* Areas 3a, 3b, and 1 of human primary somatosensory cortex. Part 2. Spatial normalization to standard anatomical space. *Neuroimage* **11**, 684–696 (2000).
33. Rademacher, J. *et al.* Variability and asymmetry in the human precentral motor system. A cytoarchitectonic and myeloarchitectonic brain mapping study. *Brain* **124**, 2232–2258 (2001).
34. Amunts, K. *et al.* Brodmann's areas 17 and 18 brought into stereotaxic space — where and how variable? *Neuroimage* **11**, 66–84 (2000).
35. Roland, P. E. *et al.* Cytoarchitectonic maps of the human brain in standard anatomical space. *Hum. Brain Mapp.* **5**, 222–227 (1997).
36. Binkofski, F. *et al.* Broca's region subserves imagery of motion: a combined cytoarchitectonic and fMRI study. *Hum. Brain Mapp.* **11**, 273–285 (2000).
37. Bodegard, A. *et al.* Object shape differences reflected by somatosensory cortical activation. *J. Neurosci.* **20**, RC51 (2000).
38. Johnsrude, I. *et al.* Cytoarchitectonic region-of-interest analysis of auditory imaging data. *Neuroimage* **13**, S897 (2001).
39. Wieshmann, U. C. *et al.* Combined functional magnetic resonance imaging and diffusion tensor imaging demonstrate widespread modified organisation in malformation of cortical development. *J. Neurol. Neurosurg. Psychiatry* **70**, 521–523 (2001).
40. Mori, S. *et al. In vivo* visualization of human neural pathways by magnetic resonance imaging. *Ann. Neurol.* **47**, 412–414 (2000).
41. Conturo, T. E. *et al.* Tracking neuronal fiber pathways in the living human brain. *Proc. Natl Acad. Sci. USA* **96**, 10422–10427 (1999).
42. Duong, T. Q. *et al.* Spatiotemporal dynamics of the BOLD fMRI signals: toward mapping submillimeter cortical columns using the early negative response. *Magn. Reson. Med.* **44**, 231–242 (2000).
43. Yoshiura, T. *et al.* Heschl and superior temporal gyri: low signal intensity of the cortex on T2-weighted MR images of the normal brain. *Radiology* **214**, 217–221 (2000).
44. Goodyear, B. G. & Menon, R. S. Brief visual stimulation allows mapping of ocular dominance in visual cortex using fMRI. *Hum. Brain Mapp.* **14**, 210–217 (2001).
45. Kanwisher, N., McDermott, J. & Chun, M. M. The fusiform face area: a module in human extrastriate cortex specialized for face perception. *J. Neurosci.* **17**, 4302–4311 (1997).
46. Epstein, R. & Kanwisher, N. A cortical representation of the local visual environment. *Nature* **392**, 598–601 (1998).
47. Downing, P. E. *et al.* A cortical area selective for visual processing of the human body. *Science* **293**, 2470–2473 (2001).
48. Epstein, R. *et al.* The parahippocampal place area: recognition, navigation, or encoding? *Neuron* **23**, 115–125 (1999).
49. Thompson, P. M. & Toga, A. W. in *Handbook of Medical Imaging: Processing and Analysis* (ed. Bankman, I.) 569–600 (Academic, San Diego, 2000).
50. Woods, R. P. *et al.* Automated image registration: II. Intersubject validation of linear and nonlinear models. *J. Comput. Assist. Tomogr.* **22**, 153–165 (1998).
51. Ashburner, J. & Friston, K. J. Nonlinear spatial normalization using basis functions. *Hum. Brain Mapp.* **7**, 254–266 (1999).
52. Fischl, B., Sereno, M. I. & Dale, A. M. Cortical surface-based analysis. II: Inflation, flattening, and a surface-based coordinate system. *Neuroimage* **9**, 195–207 (1999).
53. Thompson, P. M. *et al.* Mathematical/computational challenges in creating deformable and probabilistic atlases of the human brain. *Hum. Brain Mapp.* **9**, 81–92 (2000).
54. Jezzard, P. & Clare, S. Sources of distortion in functional MRI data. *Hum. Brain Mapp.* **8**, 80–85 (1999).
55. Woods, R. D. in *Handbook of Medical Imaging: Processing and Analysis* (ed. Bankman, I.) 491–497 (Academic, San Diego, 2000).
56. Fox, P. T., Parsons, L. M. & Lancaster, J. L. Beyond the single study: function/location metanalysis in cognitive neuroimaging. *Curr. Opin. Neurobiol.* **8**, 178–187 (1998).
57. Brett, M., Lancaster, J. & Christoff, K. Using the MNI brain with the Talairach atlas. *Neuroimage* **13**, S85 (2001).
58. Duncan, J. & Owen, A. M. Common regions of the human frontal lobe recruited by diverse cognitive demands. *Trends Neurosci.* **23**, 475–483 (2000).
59. D'Esposito, M., Postle, B. R. & Rypma, B. Prefrontal cortical contributions to working memory: evidence from event-related fMRI studies. *Exp. Brain Res.* **133**, 3–11 (2000).
60. Petersson, K. M. *et al.* Statistical limitations in functional neuroimaging II. Signal detection and statistical inference. *Phil. Trans. R. Soc. Lond. B* **354**, 1261–1281 (1999).
61. Friston, K. J. *et al.* Detecting activations in PET and fMRI: levels of inference and power. *Neuroimage* **4**, 223–235 (1996).
62. Van Horn, J. D. *et al.* Mapping voxel-based statistical power on parametric images. *Neuroimage* **7**, 97–107 (1998).
63. Andreasen, N. C. *et al.* Sample size and statistical power in [^{15}O]H_2O studies of human cognition. *J. Cereb. Blood Flow Metab.* **16**, 804–816 (1996).
64. Christoff, K. & Gabrielli, J. D. E. The frontopolar cortex and human cognition: evidence for a rostrocaudal hierarchical organization within the human prefrontal cortex. *Psychobiology* **28**, 168–186 (2000).
65. Talairach, J. & Tournoux, P. *Co-planar Stereotaxic Atlas of the Human Brain* (Thieme Medical, New York, 1988).
66. Collins, D. L. *3D Model-Based Segmentation of Individual Brain Structures from Magnetic Resonance Imaging Data.* Thesis, McGill Univ., Canada (1994).
67. Evans, A. C. *et al.* Anatomical mapping of functional activation in stereotactic coordinate space. *Neuroimage* **1**, 43–53 (1992).
68. Evans, A. C., Collins, D. L. & Milner, B. An MRI-based stereotactic atlas from 250 young normal subjects. *Soc. Neurosci. Abstr.* **18**, 408 (1992).
69. Collins, D. L. *et al.* Automatic 3D intersubject registration of MR volumetric data in standardized Talairach space. *J. Comput. Assist. Tomogr.* **18**, 192–205 (1994).
70. Duncan, J. *et al.* A neural basis for general intelligence. *Science* **289**, 457–460 (2000).

Acknowledgements
Many thanks to T. Hackett and M. Petrides for helpful discussions on cytoarchitecture, and to J. Ashburner, S. Baxendale, D. Bor, J. Collins, L. Collins, R. Cools, M. Davis, G. DiGirolamo, J. Duncan, A. Gazanfar, A. Lawrence and T. Marcel for comments on earlier drafts of this paper.

Online links

FURTHER INFORMATION
Encyclopedia of Life Sciences: http://www.els.net/
brain imaging: localization of brain functions | brain imaging: observing ongoing neural activity | magnetic resonance imaging
FSL: http://www.fmrib.ox.ac.uk/fsl/
MIT Encyclopedia of Cognitive Sciences: http://cognet.mit.edu/MITECS/
magnetic resonance imaging | positron emission tomography
MRC Cognition and Brain Sciences Unit: http://www.mrc-cbu.cam.ac.uk/
SPM99: http://www.fil.ion.ucl.ac.uk/spm/
Access to this interactive links box is free online.